

# Intramolecular energy transfer and luminescence enhancement effect in inert rare earth ions (La, Y, Gd)–Eu<sup>3+</sup> (Tb<sup>3+</sup>) co-fabricated organic–inorganic hybrid materials by covalent grafting

Fang-fang Wang<sup>a</sup>, Bing Yan<sup>a,b,\*</sup>

<sup>a</sup> Department of Chemistry, Tongji University, Siping Road 1239, Shanghai 200092, China

<sup>b</sup> State Key Lab of Rare Earth Materials Chemistry and Applications, Peking University, Beijing 100871, China

Received 17 April 2007; received in revised form 19 July 2007; accepted 21 August 2007

Available online 24 August 2007

## Abstract

In this paper, a novel kind of organic–inorganic monomer, HIPA-TESPIC, has been achieved by modifying 5-hydroxyisophthalic acid (abbreviated as HIPA) with 3-(triethoxysilyl)-propyl isocyanate (abbreviated as TESPIC). The organic–inorganic monomers (HIPA-TESPIC) with two components equipped with covalent bonds can behave as a functional molecular bridge, which can not only coordinate to RE ions but also occur in situ sol–gel process with inorganic host precursor tetraethoxysilane (TEOS), resulting a kind of molecular hybrid material (named as RE-HIPA-TESPIC) with double chemical bond (RE–O coordination bond and Si–O covalent bond). <sup>1</sup>H NMR, Fourier transform infrared (FT-IR) were applied to characterize the structure of HIPA-TESPIC and UV–vis spectrophotometer, phosphorescence, and luminescence spectra were applied to characterize the photophysical properties of the obtained hybrid material. Luminescent hybrid materials consisting of active rare earth ions (Tb<sup>3+</sup>, Eu<sup>3+</sup>)–inert rare earth ions (Y<sup>3+</sup>, La<sup>3+</sup>, Gd<sup>3+</sup>) complex covalently bonded to a silica-based network have been obtained in situ via a sol–gel approach. Through co-hydrolysis and polycondensation, active rare earth ions and inert rare earth ions can be introduced in the same organic–inorganic hybrid monomer and then formed Si–O backbones. The luminescent behavior has been studied with the different ratios of active rare earth ions–inert rare earth ions, which suggests that the existence of inert rare earth ions can enhance the luminescence intensity, which may be due to the intramolecular energy transfer between inert rare earth ions and active rare earth ions.

© 2007 Elsevier B.V. All rights reserved.

**Keywords:** Luminescence enhancement; Intramolecular energy transfer; Molecular hybrid materials; Covalently bonded

## 1. Introduction

With the expansion of soft inorganic chemistry processes, the synthesis of inorganic–organic hybrid systems appeared over the past decade, which possessed of the mutual advantages of both organic and inorganic networks and has been applied widely in many fields [1,2]. Among all the synthetic methods, the sol–gel approach which is based on co-hydrolysis/polycondensation reactions of metal alkoxides exhibits a wealth of unique characteristics, namely, convenience, low temperature, and versatility [3–8]. Generally speaking, hybrids of rare earth organic complexes introduced in silica gel have already been found to display characteristic emission intensities compared with rare earth ions

in inorganic hosts, and organic components are considered to be efficient sensitizers for the luminescence of rare earth ions, at a word, the antenna effect, which solve the problem of the very low absorption coefficients of the rare earth ions. With respect to the inorganic–organic hybrids, the definition is quite wide and several attempts have been made to achieve a classification of these new materials according to their structural properties. Following the classification by Sanchez and Ribot [9], the inorganic–organic hybrids can be divided into two major classes according to interaction among the different components or phases in hybrid systems [10]. For class I hybrid materials, the organic and inorganic components are connected by only the weak functional interactions (such as hydrogen bonding, van der Waals force or static effect) between the organic and inorganic components, and it seems impossible to solve the problems of uneven distribution of rare earth complexes, limitation of doped concentration, quenching effect of luminescent centers,

\* Corresponding author.

E-mail address: [byan@tongji.edu.cn](mailto:byan@tongji.edu.cn) (B. Yan).

separation of different phases, which can be ascribed to the only weak functional interactions [11–14]. But for class II hybrid materials, the two components are connected by covalent grafting, which can achieve true interconnection between the organic and inorganic moieties and successfully solve the above-mentioned problems. In nature, the organic components play a role of network modifier, which can not only realize the possibility of molecular-based material but also tailor the complementary properties of novel multifunctional advanced materials through covalent grafting between the different components [15]. Lately, a few researches which concerned the covalently bonded hybrids have emerged and the as-derived molecular-based materials present monophasic appearance even at a high concentration of rare earth complexes [16–22]. So the key to prepare the class II hybrid materials is to synthesize an intermediate as a covalent bridge, which can not only coordinate to RE ions but also act as precursors of inorganic network.

Inorganic matrices doped with metal complexes especially rare earth complexes are attractive materials for optical applications owing to their excellent luminescence characteristics from the electronic transitions between the 4f energy levels. But by far there were only a few studies to be unfolded on emission properties of trivalent rare earth ions incorporated inside room-temperature sol–gel matrices, and they focus their interest mainly on single rare earth hybrids [12,16,22,23,24,25,26]. Some researches have been carried out since research worker found that all of the enhancing ions have a stable electronic configuration, such as  $\text{La}^{3+}$ ,  $\text{Y}^{3+}$ ,  $\text{Gd}^{3+}$  and  $\text{Lu}^{3+}$ , the 4f shells of which were empty, half-filled and full, respectively [27–29]. But these researches concentrated on the RE complexes in which luminescence enhancement mainly belongs to intermolecular energy transfer because it is hard to clearly prove they are homogenous and pure molecular level. Because of intermolecular energy transfer, the effect of luminescence enhancement cannot reach people's expectation. So, in this paper, we studied the mechanism of co-luminescence, which was excited by intramolecular energy transfer. We synthesized a series of molecular hybrid materials, in which the nitrate of inert rare earth, such as  $\text{Gd}^{3+}$ ,  $\text{La}^{3+}$  and  $\text{Y}^{3+}$ , and the nitrate of active rare earth, such as  $\text{Tb}^{3+}$ ,  $\text{Eu}^{3+}$ , were mixed with different ratios and then the mixture added in the sol–gel matrices, and the hybrids showed excellent emission intensity. Because the inert rare earth and active rare earth ions combined with the silica-based network through the same co-hydrolysis and polycondensation process, then they co-exist in the same silica-based molecular Si–O network and intramolecular energy transfer can occur. In order to characterize the structure of intermediate, Fourier transform infrared (FT-IR), UV–vis spectrophotometer,  $^1\text{H}$  NMR were used, the photophysical properties were discussed in detail.

## 2. Experiment

### 2.1. Materials

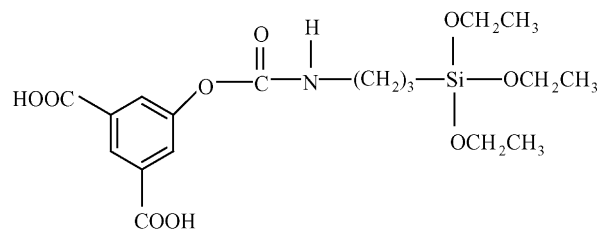
5-hydroxyisophthalic acid (abbreviated as HIPA) and 3-(triethoxysilyl)-propyl isocyanate (abbreviated as TESPIC) were supplied by Lancaster Synthesis Ltd. Solvents used were

purified by common methods. Other starting reagents were used as received.

### 2.2. Synthesis of organic–inorganic intermediate

A typical procedure for the preparation of organic–inorganic intermediate (HIPA-TESPIC) was as follows: 2 mmol 5-hydroxyisophthalic acid (0.364 g) was first dissolved in acetone by stirring and 2 mmol 3-(triethoxysilyl)-propyl isocyanate (0.495 g) was then added to the solution by drops. The whole mixture was refluxed at  $65^\circ\text{C}$  under argon atmosphere for 12 h. After isolation, a white powder of HIPA-TESPIC was obtained. The typical procedure was according to the reaction scheme in Fig. 1 and the spectra of FT-IR are seen in Fig. 3; HIPA-TESPIC ( $\text{C}_{18}\text{H}_{27}\text{NO}_9\text{Si}$ ): Element analysis data: *Anal.* Calcd.: C, 50.40; H, 6.33; N, 3.26. Found: C, 50.61; H, 6.16; N, 3.08.  $^1\text{H}$  NMR are as follows, HIPA-TESPIC ( $\text{C}_{18}\text{H}_{27}\text{O}_9\text{NSi}$ ):  $^1\text{H}$  NMR (DMSO) d (ppm): 8.21 (1H, s), 7.92 (1H, s), 7.51 (2H, s), 3.70 (6H, q), 3.41 (2H, q), 1.47 (2H, m), 1.01 (9H, t), 0.51 (2H, t).

The scheme for the molecular composition is shown below.



### 2.3. Sol–gel polymerizations

Sol–gel derived hybrid material containing rare earth was prepared as follows: the synthesized precursor HIPA-TESPIC was dissolved in dimethylformamide (DMF), then tetraethoxysilane (TEOS), which actually allowed a better miscibility of rare earth nitrate solution to the reaction mixture and increased the degree of cross-linking and the total silica content, and  $\text{H}_2\text{O}$  was added while stirring, and then one drop of diluted hydrochloric acid was added to promote hydrolysis. A stoichiometric amount of  $\text{RE}^{3+}$  (a different ratio blend of active rare earth ions nitrate and inert rare earth ions nitrate) was added to the final stirring mixture. The mole ratio of  $\text{RE}^{3+}$ /HIPA-TESPIC/TEOS/ $\text{H}_2\text{O}$  was 1:3:6:24. After the treatment of hydrolysis, an appropriate amount of hexamethylene-tetramine was added to adjust the PH value to about 6.5. The mixture was stirred to achieve a single phase and thermal treatment was performed at  $60^\circ\text{C}$  until the sample solidified. Using the same method, we also prepared active rare earth ions and inert rare earth ions co-hybrid materials by mixing active rare earth ions and inert rare earth ions at different ratios ( $\text{Gd}^{3+}:\text{Tb}^{3+} = 3:1, 2:1, 1:1, 1:2, 1:3$ ;  $\text{La}^{3+}:\text{Tb}^{3+} = 3:1, 2:1, 1:1, 1:2, 1:3$ ;  $\text{Y}^{3+}:\text{Tb}^{3+} = 3:1, 2:1, 1:1, 1:2, 1:3$ ;  $\text{Gd}^{3+}:\text{Eu}^{3+} = 3:1, 2:1, 1:1, 1:2, 1:3$ ;  $\text{La}^{3+}:\text{Eu}^{3+} = 3:1, 2:1, 1:1, 1:2, 1:3$ ;  $\text{Y}^{3+}:\text{Eu}^{3+} = 3:1, 2:1, 1:1, 1:2, 1:3$ ) and denoted these as hybrid31, hybrid21, hybrid11, hybrid12, hybrid13, respectively. For the purpose of comparison, we also prepared hybrid material directly with  $\text{Tb}^{3+}/\text{Eu}^{3+}$ . The hybrid material prepared with  $\text{Tb}^{3+}$  and  $\text{Eu}^{3+}$  was denoted as hybrid  $\text{Tb}^{3+}$  and hybrid

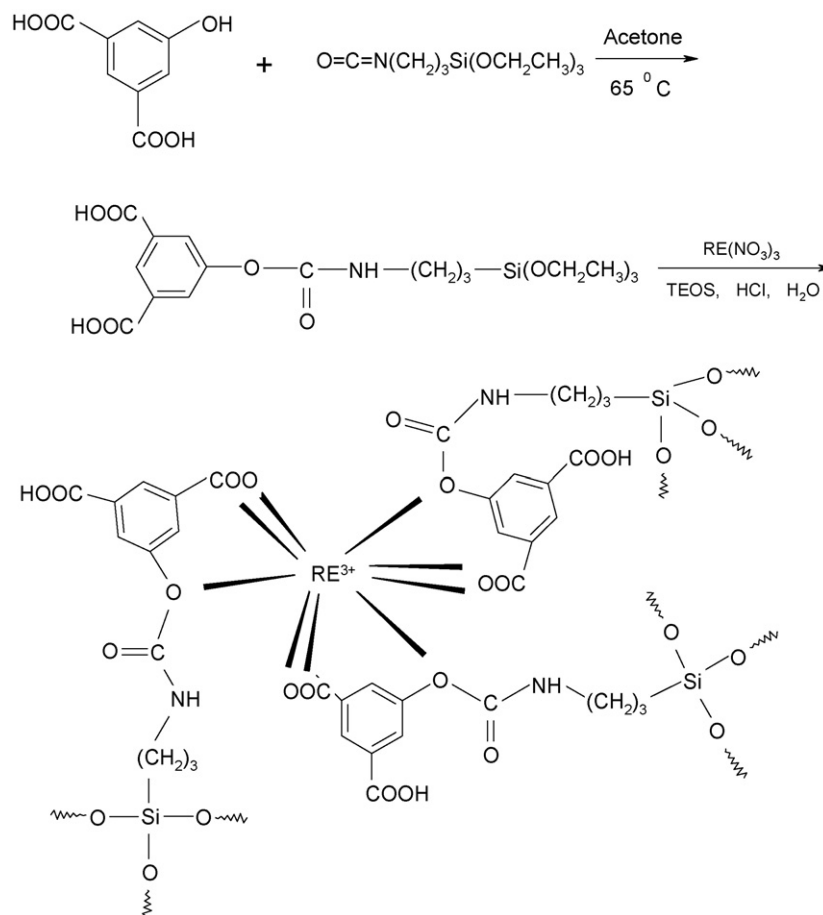


Fig. 1. Scheme of the synthesis process of HIPA-TESPIC ligand and predicted structure of resulting hybrid systems.

Eu<sup>3+</sup>. The structure for the final hybrid is shown in Fig. 2. In order to compare the luminescent lifetimes, we also prepared the Eu and Tb hybrids without inert rare earth ions.

#### 2.4. Characterization

Infrared spectroscopy was obtained in KBr pellets and recorded on a Nexus 912 AO446 FT-IR spectrophotometer in the range of 4000–400 cm<sup>-1</sup>. <sup>1</sup>H NMR spectra were recorded in DMSO on a Bruker AVANCE-500 spectrometer with tetramethylsilane (TMS) as internal reference. Ultraviolet absorption spectra of these power samples (5 × 10<sup>-4</sup> mol L<sup>-1</sup> dimethylformamide (DMF) solution) were recorded with an Agilent 8453 spectrophotometer. Phosphorescence spectra (5 × 10<sup>-4</sup> mol L<sup>-1</sup> DMF solution) and luminescence excitation and emission spectra were obtained on a Perkin-Elmer LS-55 spectrophotometer: excitation slit width = 1.5 nm, emission slit

width = 3.0 nm. Luminescent lifetimes for hybrid materials were obtained with an Edinburgh Instruments FLS 920 phosphorimeter using a 450 W xenon lamp as excitation source (pulse width, 3 μs). All measurements were completed under room temperature except for phosphorescence spectra which were measured at 77 K.

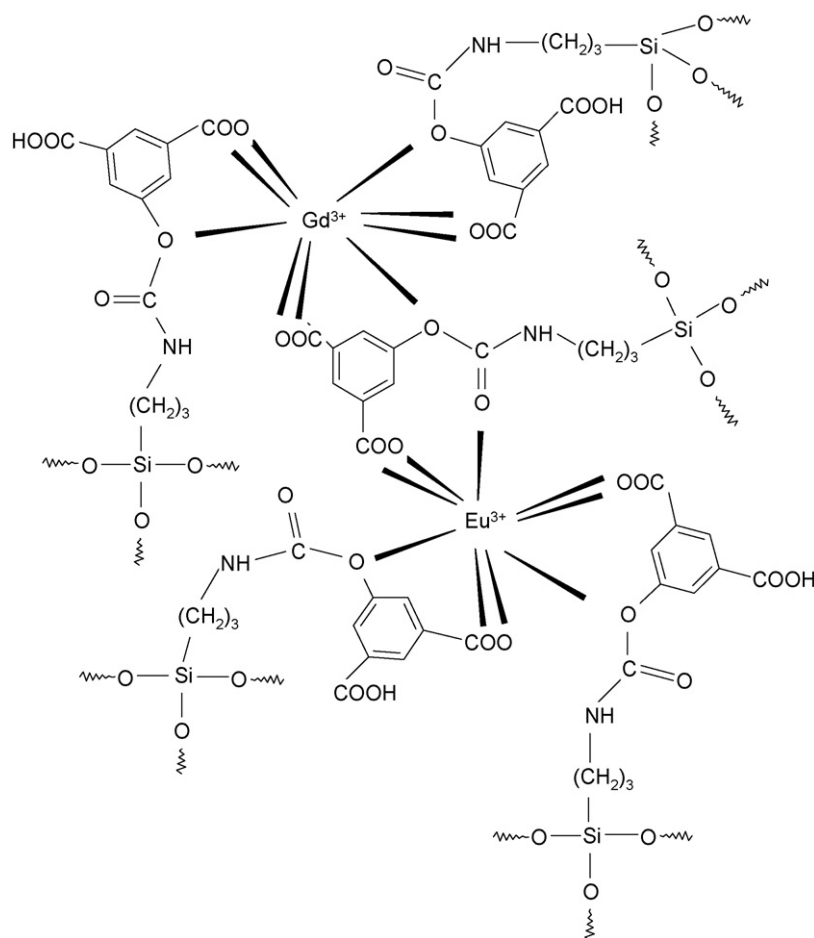
### 3. Results and discussion

#### 3.1. Formation of hybrid molecular materials

The IR spectra of HIPA, TESPIC and the modified bridge HIPA-TESPIC were compared, and the main absorption and their assignments are shown in Fig. 3 and Table 1. The formation of acylamino group and Si–O–Si network can be proved by this figure. Compared the IR spectra of HIPA-TESPIC with HIPA and TESPIC, the appearance of the bands located at around

Table 1  
The main bands and their assignments of IR spectra for HIPA, TESPIC, HIPA-TESPIC

Compounds	ν(C=O) (cm <sup>-1</sup> )	ν(N=C=O) (cm <sup>-1</sup> )	δ(N–H) (cm <sup>-1</sup> )	ν(C–N) (cm <sup>-1</sup> )	ν(Si–O) (cm <sup>-1</sup> )	ν(Si–C) (cm <sup>-1</sup> )
HIPA	1704	–	–	–	–	–
TESPIC	1630	2266	–	–	1077	1164
HIPA-TESPIC	1685	–	1521	1408	1078	1165

Fig. 2. Schematic illustration of  $\text{Eu}^{3+}$ – $\text{Gd}^{3+}$  co-hybrids.

$1685\text{ cm}^{-1}$  due to the absorption of amide groups (CONH) and the presence of the bending vibration ( $\delta_{\text{NH}}$ ,  $1408\text{ cm}^{-1}$ ) suggested that 3-(triethoxysilyl)-propyl isocyanate has been successfully grafted onto 5-hydroxyisophthalic acid. The stretching

vibration ( $\nu_{\text{Si-O}}$ ) located at around  $1078\text{ cm}^{-1}$  and the stretching vibration ( $\nu_{\text{Si-C}}$ ) located at  $1165\text{ cm}^{-1}$  existed in the IR spectra of bridge molecule (HIPA-TESPIC) compared with the IR spectra of HIPA, which is the evidence of the emer-

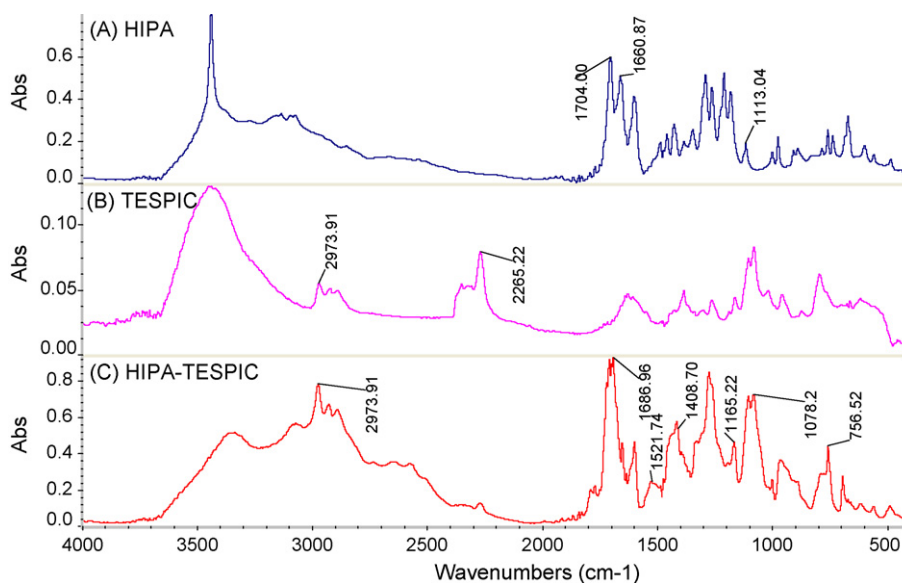


Fig. 3. FT-IR spectra of (A) HIPA, (B) TESPIC and (C) HIPA-TESPIC.

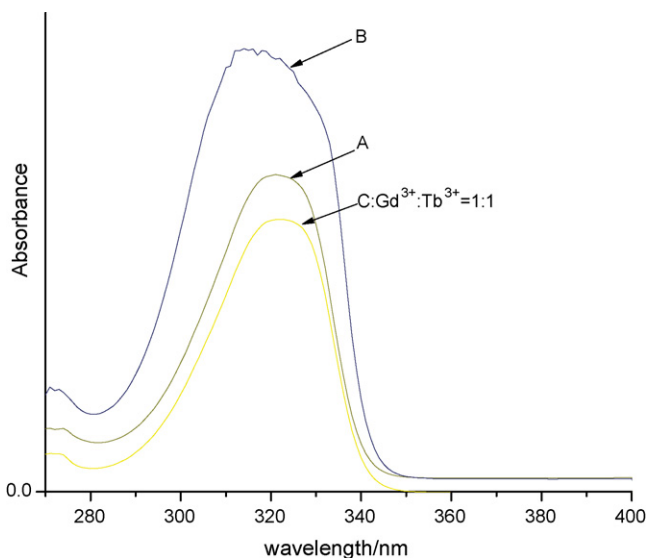


Fig. 4. Ultraviolet absorption spectra of (A) HIPA, (B) HIPA-TESPIC and (C) hybrid  $\text{Gd}^{3+}:\text{Tb}^{3+} = 1:1$ .

gence of HIPA-TESPIC. In addition, the absorption peak at  $2273\text{--}2378\text{ cm}^{-1}$  for  $\text{N}=\text{C}=\text{O}$  disappeared in the I.R. spectra of HIPA-TESPIC, which indicated the occurrence of the covalent grafting reaction.

In addition, the  $^1\text{H}$  NMR spectroscopy can also explain the structure of HIPA-TESPIC. For the  $^1\text{H}$  NMR spectroscopy of HIPA-TESPIC, the peaks at chemical shifts of about 7.92, 7.51 ppm correspond to the H of the aromatic ring. The chemical shift of 8.21 ppm belongs to the H of NH, 3.70 ppm belongs to  $-\text{O}-\text{CH}_2-$  and 0.51 ppm belongs to  $-\text{CH}_2-\text{Si}-$ .

Fig. 4 shows ultraviolet absorption spectra of (A) HIPA, (B) HIPA-TESPIC and (C) hybrid  $\text{Gd}^{3+}:\text{Tb}^{3+} = 1:1$ . From the spectra, we found a blue shift of the major  $\pi-\pi^*$  electronic transitions (from 320 to 314 nm), indicating that modification of 5-hydroxyisophthalic acid, which was grafted by 3-(triethoxysilyl)-propyl isocyanate, influenced its corresponding absorption spectrum. Furthermore, an obvious red shift is observed when we add  $\text{RE}^{3+}$  to HIPA-TESPIC (from 314 to 322 nm), which is probably due to formation of a complex between  $\text{RE}^{3+}$  and HIPA-TESPIC.

### 3.2. Phosphorescence spectra

Fig. 5 shows the low-temperature phosphorescence spectra of (A) hybrid  $\text{Tb}^{3+}$ , (B) hybrid  $\text{Gd}^{3+}:\text{Tb}^{3+} = 1:1$ , (C) hybrid  $\text{Y}^{3+}:\text{Tb}^{3+} = 1:1$ , (D) hybrid  $\text{La}^{3+}:\text{Tb}^{3+} = 1:1$  at 77 K. As we all know, phosphorescence spectrum indicates the character of the organic molecular ligands and different phosphorescence bands correspond to diverse ligand molecules, so there is no change between organic and inorganic intermediates and hybrids with only the difference of their intensities for the same HIPA-TESPIC ligand group [30]. According to the intramolecular energy transfer mechanism, the corresponding intramolecular transfer efficiency from the HIPA-TESPIC to  $\text{Tb}^{3+}$  mainly depends on the energy match between the triplet state energy of HIPA-TESPIC (corresponding to the phospho-

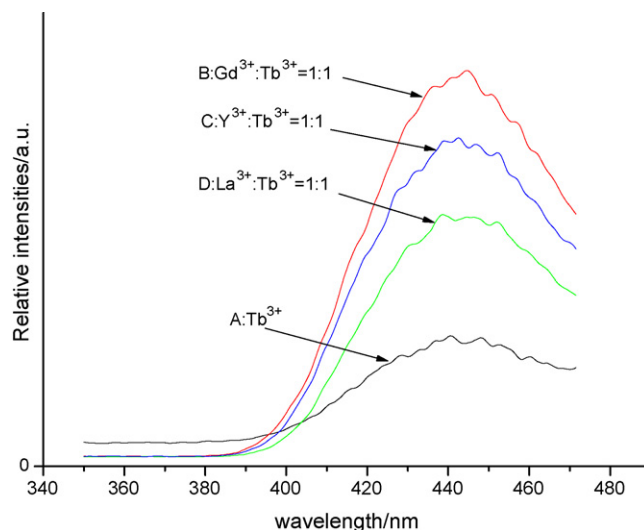


Fig. 5. The phosphorescent spectra of (A) hybrid  $\text{Tb}^{3+}$ , (B) hybrid  $\text{Gd}^{3+}:\text{Tb}^{3+} = 1:1$ , (C) hybrid  $\text{Y}^{3+}:\text{Tb}^{3+} = 1:1$  and (D) hybrid  $\text{La}^{3+}:\text{Tb}^{3+} = 1:1$ .

rescence band) and the resonant emissive energy level of the central  $\text{Tb}^{3+}$  (approximately  $4000 \pm 500\text{ cm}^{-1}$ ). From the figure, it can be seen that the former energy level corresponds to a peak at 444 nm and equals  $22500\text{ cm}^{-1}$ ; likewise the latter is  $20400\text{ cm}^{-1}$  (490 nm,  $^5\text{D}_4 \rightarrow ^7\text{F}_6$  transition). Therefore, it can be predicted that HIPA-TESPIC shows a good energy match and sensitizes the luminescence of  $\text{Tb}^{3+}$  in terms of the inverse energy transfer theory. Furthermore, from this figure, it can be seen that the phosphorescence intensity of hybrid 11 is strengthened compared with hybrid  $\text{Tb}^{3+}$  while a red shift or blue shift does not occur when inert rare earth ions ( $\text{Gd}^{3+}$ ,  $\text{Y}^{3+}$ ,  $\text{La}^{3+}$ ) are added. So we can get such a conclusion that the inert ions ( $\text{Gd}^{3+}$ ,  $\text{Y}^{3+}$ ,  $\text{La}^{3+}$ ) can strengthen the efficiency of luminescence.

### 3.3. Luminescent properties

On the basis of luminescence enhancement effect of active rare earth ions (such as  $\text{Eu}^{3+}$  or  $\text{Tb}^{3+}$ ) brought by inert rare earth ions (i.e.  $\text{La}^{3+}$ ,  $\text{Ga}^{3+}$ ,  $\text{Lu}^{3+}$ ,  $\text{Y}^{3+}$ ) in solution systems or solid complexes, we intercalated different ratios of active rare earth ions ( $\text{Eu}^{3+}$  or  $\text{Tb}^{3+}$ ) and inert rare earth ions ( $\text{La}^{3+}$ ,  $\text{Ga}^{3+}$ ,  $\text{Y}^{3+}$ ) into the hybrid molecular materials with chemical bonded Si–O network after the co-hydrolysis and co-polycondensation process. The excitation spectra for the  $\text{Y}^{3+}-\text{Eu}^{3+}$  co-doped hybrids are shown in Fig. 6. The excitation spectra were obtained by monitoring the emission of the  $\text{Eu}^{3+}$  at 613 nm, and all the systems have similar excitation spectra that are dominated by a broad band from 388 to 403 nm with the maximum peak at about 393 nm, which is attributed to the f–f transition of  $\text{Eu}(\text{III})$  ion. The emission spectra for the  $\text{Y}^{3+}-\text{Eu}^{3+}/\text{Gd}^{3+}-\text{Eu}^{3+}/\text{La}^{3+}-\text{Eu}^{3+}$  co-doped hybrids are shown in Fig. 7. The emission lines of hybrid material are assigned to the characteristic  $^5\text{D}_0 \rightarrow ^7\text{F}_1$  and  $^5\text{D}_0 \rightarrow ^7\text{F}_2$  transitions of  $\text{Eu}^{3+}$  at 588 and 613 nm, respectively, while the emission lines of  $^5\text{D}_0 \rightarrow ^7\text{F}_3$  and  $^5\text{D}_0 \rightarrow ^7\text{F}_4$  are too weak to be observed. The fluorescence intensity at 613 nm is the strongest for the  $^5\text{D}_0-^7\text{F}_2$



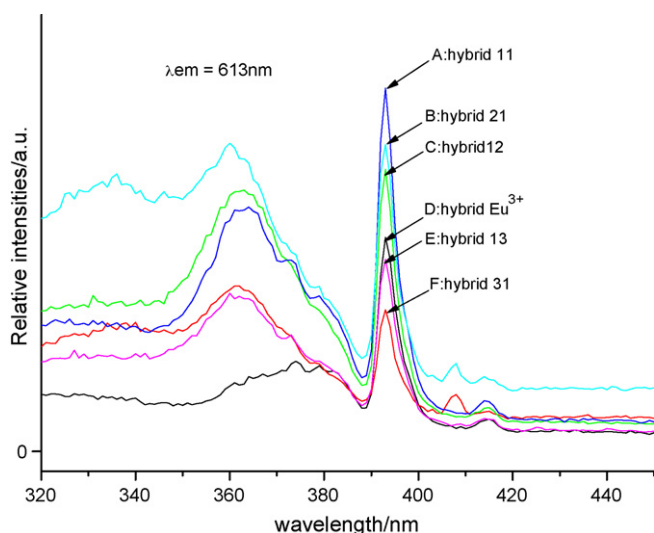


Fig. 6. Excitation spectra of (A) hybrid 11, (B) hybrid 21, (C) hybrid 12, (D) hybrid  $\text{Eu}^{3+}$ , (E) hybrid 13 and (F) hybrid 31 for the  $\text{Y}^{3+}$ - $\text{Eu}^{3+}$  co-doped hybrids.

emission which is the most prominent one. From the excitation spectrum, when  $\text{Y}^{3+}$  ( $\text{Gd}^{3+}$  or  $\text{La}^{3+}$ ): $\text{Eu}^{3+} = 1:1$ , the intensity of the spectrum was stronger than others. Corresponding to the excitation spectrum, the fluorescent intensities of hybrids changed with the same sequence.

The excitation spectra for the  $\text{Y}^{3+}$ - $\text{Tb}^{3+}$  co-doped hybrids are shown in Fig. 8. The excitation spectra were obtained by monitoring the emission of the  $\text{Tb}^{3+}$  at 543 nm, and all the systems presented a broad band at the range of 274–380 nm, centered at 322 and 356 nm, respectively, which indicate that the HIPA-TESPIC created the extensive localized system for the effective energy absorption to sensitize the luminescence of  $\text{Tb}^{3+}$ . The emission spectra for the  $\text{Y}^{3+}$ - $\text{Tb}^{3+}$ / $\text{La}^{3+}$ - $\text{Tb}^{3+}$ / $\text{Gd}^{3+}$ - $\text{Tb}^{3+}$  co-doped hybrids are shown in Fig. 9. The emission lines of hybrid material are assigned to the characteristic  $^5\text{D}_4$ - $^7\text{F}_J$  ( $J = 6, 5, 4, 3$ ) transitions of  $\text{Tb}^{3+}$  at 488, 543, 583 and 619 nm respectively, and the fluorescence intensity at 543 nm is the strongest for the  $^5\text{D}_4$ - $^7\text{F}_5$  emission which is the most prominent one. The flo-

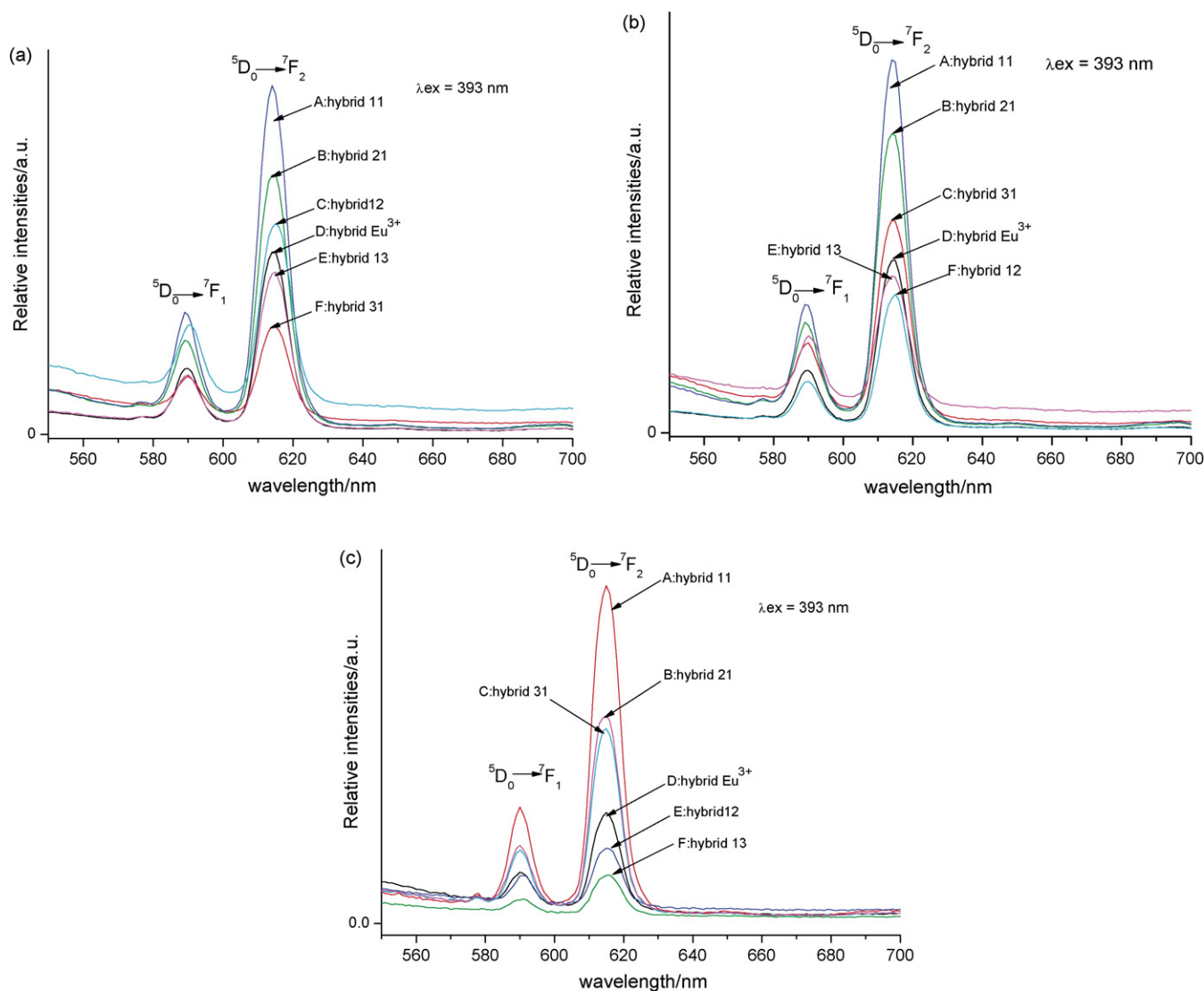


Fig. 7. (a) Emission spectra of (A) hybrid 11, (B) hybrid 21, (C) hybrid 12, (D) hybrid  $\text{Eu}^{3+}$ , (E) hybrid 13 and (E) hybrid 31 for the  $\text{Y}^{3+}$ - $\text{Eu}^{3+}$  co-doped hybrids (b) Emission spectra of (A) hybrid 11, (B) hybrid 21, (C) hybrid 12, (D) hybrid  $\text{Eu}^{3+}$ , (E) hybrid 13 and (E) hybrid 31 for the  $\text{Gd}^{3+}$ - $\text{Eu}^{3+}$  co-doped hybrids (c) Emission spectra of (A) hybrid 11, (B) hybrid 21, (C) hybrid 12, (D) hybrid  $\text{Eu}^{3+}$ , (E) hybrid 13 and (E) hybrid 31 for the  $\text{La}^{3+}$ - $\text{Eu}^{3+}$  co-doped hybrids.

Table 2  
The luminescent lifetimes of selected hybrid materials

Hybrids	Eu hybrids	Eu <sup>3+</sup> –Y <sup>3+</sup> co-hybrid11	Eu <sup>3+</sup> –Gd <sup>3+</sup> co-hybrid11	Eu <sup>3+</sup> –La <sup>3+</sup> co-hybrid11	Tb hybrids	Tb <sup>3+</sup> –Y <sup>3+</sup> co-hybrid11	Tb <sup>3+</sup> –Gd <sup>3+</sup> co-hybrid11	Tb <sup>3+</sup> –La <sup>3+</sup> co-hybrid11
Lifetimes (μs)	1040	1380	1220	1295	1175	1605	1540	1460

rescence intensity at 543 nm is the strongest for the <sup>5</sup>D<sub>4</sub>–<sup>7</sup>F<sub>5</sub> emission which is the most prominent one. From the excitation spectrum, when Y<sup>3+</sup> (Gd<sup>3+</sup> or La<sup>3+</sup>):Tb<sup>3+</sup> = 1:1, the intensity of the spectrum was stronger than others. Corresponding to the excitation spectrum, the fluorescent intensities of hybrids changed with the same sequence.

Although HIPA can sensitize active rare earth ions (Eu<sup>3+</sup>, Tb<sup>3+</sup>) and hybrid Eu<sup>3+</sup>/Tb<sup>3+</sup> can exhibit good luminescence characteristic, its intensity was not strong. However, the luminescence intensity of hybrids is much enhanced when inert rare earth ions were added to the hybrid Eu<sup>3+</sup> (Tb<sup>3+</sup>); and this is a newly found co-luminescence system. Strong emission intensity and narrow half emission width (below 15 nm) were observed, which show the luminescence characteristics of the resulting hybrid materials.

Further, we measured the luminescent lifetimes of selected hybrids, which are shown in Table 2. The luminescent lifetimes are longer than general rare earth complexes whose lifetimes are mostly shorter than 1000 μs, suggesting the molecular hybrids with strong chemical bonds enhance the luminescent stability. Besides, the luminescent lifetimes of cohybrids fabricated with inert rare earth ions are longer than those of pure Eu or Tb hybrids. The introduction of inert RE<sup>3+</sup> ions (Y<sup>3+</sup>, Gd<sup>3+</sup>, La<sup>3+</sup>) decreased the non-radiative deactivation energy transfer process, resulting in the enhancement of luminescent lifetimes.

### 3.4. Luminescence mechanism

When the rare earth mixture composed of active rare earth ions (Eu<sup>3+</sup>, Tb<sup>3+</sup>) and inert rare earth ions (Gd<sup>3+</sup>, Y<sup>3+</sup>, La<sup>3+</sup>) in

appropriate ratio was added to the silica-based molecular hybrid materials, the characteristic emission bands of active rare earth ions (Eu<sup>3+</sup>, Tb<sup>3+</sup>) were much enhanced. The mechanism of this luminescence enhancement effect is as follows. As we all know, HIPA can absorb radiant energy and then transfer it to active rare earth ions (Eu<sup>3+</sup>, Tb<sup>3+</sup>). Because the rare earth nitrates can hydrolyze and polymerize together with HIPA-TESPIC and TEOS, we considered that active rare earth ions and inert rare earth ions coexist in the same molecular hybrids at molecular degree through the chemical bonded Si–O network. It can be presumed that the intramolecular energy transfer occurs and the transfer process from the energy donor (HIPA) to Tb<sup>3+</sup> is enhanced, which agrees with the similar phenomenon in other systems [27]. In this sort of co-luminescence system, because the inert RE complexes and the active RE complexes are in the same molecule and the distance between them is very small, so the inert RE ions can act as a energy bridge through which the energy of HIPA-TESPIC in the inert RE complexes can be transferred to the active rare earth ions (Eu<sup>3+</sup>, Tb<sup>3+</sup>) through intramolecular energy transfer, which lead to the enhanced luminescence of Tb<sup>3+</sup> in the hybrids. In addition, from Fig. 2, we can see that the concentration of inert rare earth ions is great enough and each of Eu-HIPA-TESPIC molecular fragments is surrounded by many Gd-HIPA-TESPIC molecular fragments. These Gd-HIPA-TESPIC molecular fragments can form a cage which acts as an energy-insulating sheath to prevent collision with water molecules and decrease the energy loss of Eu-HIPA-TESPIC, thus luminescence quantum efficiency and luminescence intensity are improved.

Furthermore, from Figs. 7 and 9, the characteristic emission of inert rare earth ions (Gd<sup>3+</sup>, Y<sup>3+</sup>, La<sup>3+</sup>) is not observed. This is probably due to the fact that inert rare earth ions possesses a relatively stable 4f shell and the excited state of inert rare earth ions is higher than the triplet start of HIPA-TESPIC, so the energy of HIPA-TESPIC cannot be transferred to inert rare earth ions by an intramolecular energy transfer process, and the emission of co-doped hybrids are ascribed to direct excitation of the Eu(III) ion or Tb(III) ion.

### 3.5. SEM image

Fig. 10 shows the selected scanning electron micrographs for the molecular hybrid Gd<sup>3+</sup>–Tb<sup>3+</sup> (1:1). From the scanning electron micrograph, we can see no phase separation, which demonstrates that a homogeneous, molecular-based system was obtained because of strong covalent bonds bridging between the inorganic and organic phases which belongs to a complicated huge molecule in nature. So we can conclude that the hybrid Gd<sup>3+</sup>–Tb<sup>3+</sup> (1:1) is apt to grow into infinite chainlike structure from the microstructure view and retain the coordi-

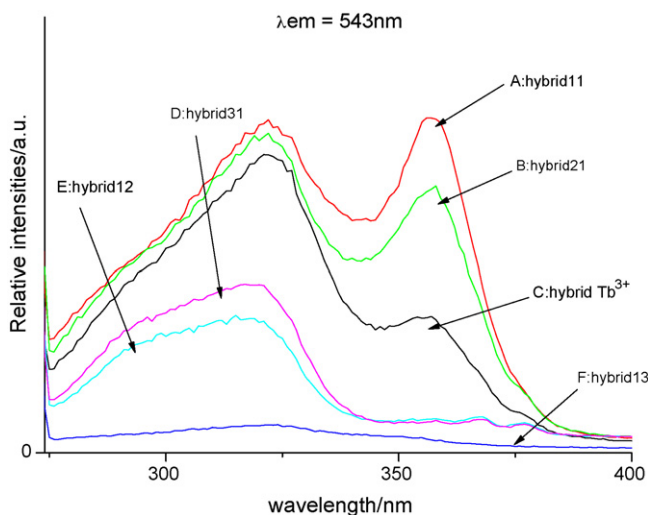


Fig. 8. Excitation spectrum of (A) hybrid 11, (B) hybrid 21, (C) hybrid 12, (D) hybrid Tb<sup>3+</sup>, (E) hybrid 13 and (F) hybrid 31 for the Y<sup>3+</sup>–Tb<sup>3+</sup> co-doped hybrids.

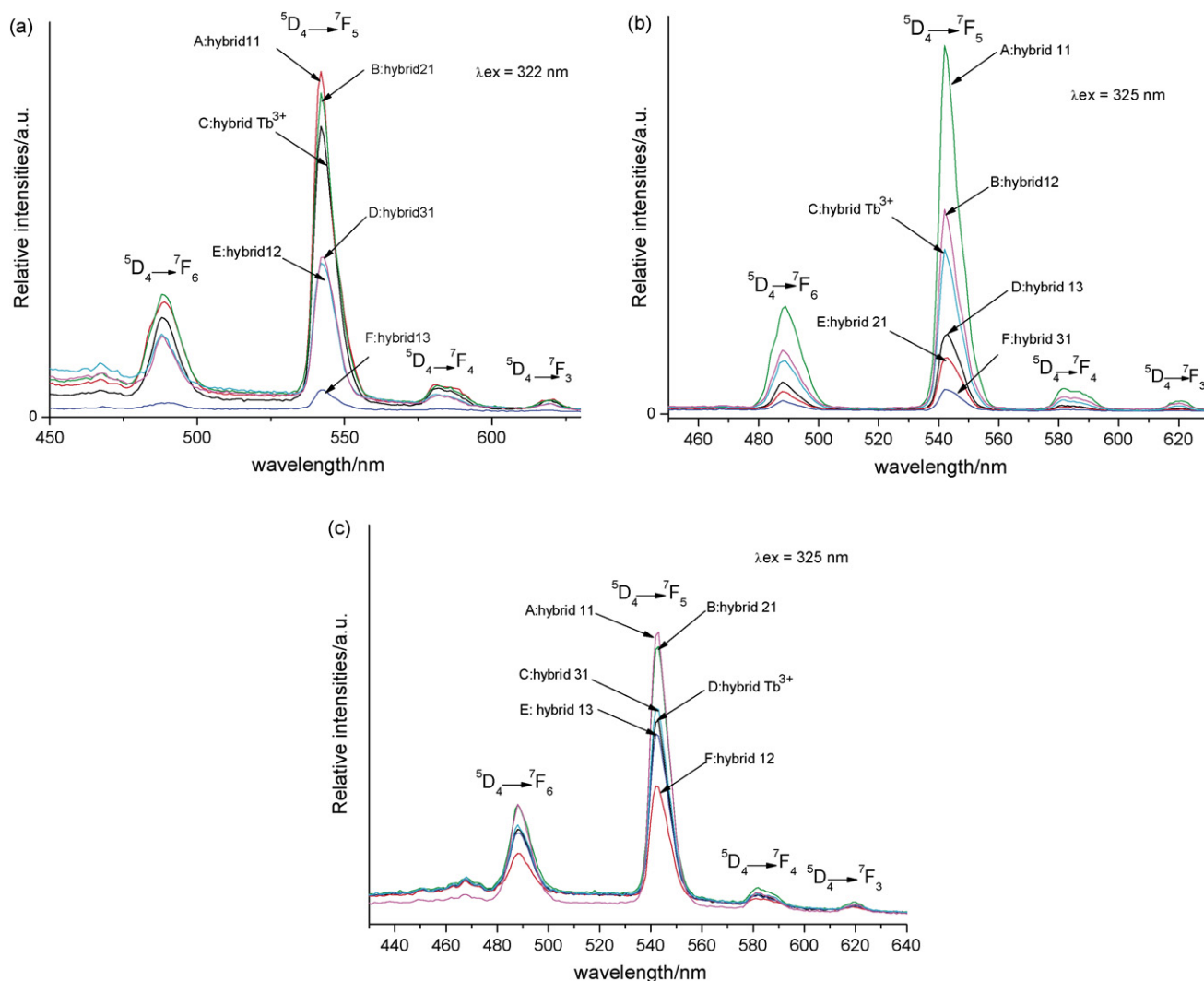


Fig. 9. (a) Emission spectra of (A) hybrid 11, (B) hybrid 21, (C) hybrid 12, (D) hybrid  $\text{Tb}^{3+}$ , (E) hybrid 13 and (E) hybrid 31 for the  $\text{Y}^{3+}$ - $\text{Tb}^{3+}$  co-doped hybrids (b) Emission spectra of (A) hybrid 11, (B) hybrid 21, (C) hybrid 12, (D) hybrid  $\text{Tb}^{3+}$ , (E) hybrid 13 and (E) hybrid 31 for the  $\text{La}^{3+}$ - $\text{Tb}^{3+}$  co-doped hybrids (c) Emission spectra of (A) hybrid 11, (B) hybrid 21, (C) hybrid 12, (D) hybrid  $\text{Tb}^{3+}$ , (E) hybrid 13 and (E) hybrid 31 for the  $\text{Gd}^{3+}$ - $\text{Tb}^{3+}$  co-doped hybrids.

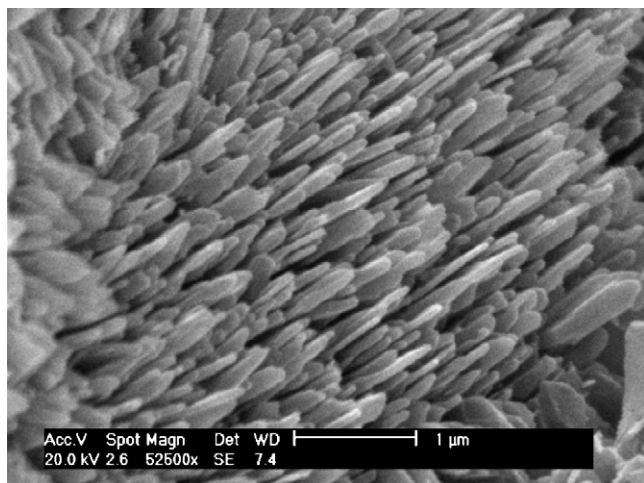


Fig. 10. SEM micrographs of  $\text{Gd}^{3+}$ - $\text{Tb}^{3+}$  co-doped (1:1) molecular-based hybrid.

nated positions in corresponding bulk materials. In the process of co-hydrolysis and polycondensation, the structure of hybrids can be formed according to different kinds of competitive mechanism. The first one is the tendency to form the one-dimensional chain-like structure which due to the ligand is composed of 5-hydroxyisophthalic acid, and the second one is the tendency to form the polymeric network structure of Si-O, but the first one plays a primary role. So in this way, the trunk structure was achieved for the dominant growth along the terbium coordination polymer chain in the former, while the latter formed normally homogeneous materials.

#### 4. Conclusion

In summary, we have designed molecular-based hybrid systems with crosslinking reagent derivatives (TESPIC) and 5-hydroxyisophthalic acid, and successfully gained a functional bridge molecule which plays double roles. On the one hand, it can coordinate to rare earth ions through carbonyl groups; on



the other hand, the hydrolysis and polycondensation reactions between triethoxysilyl of HIPA-TEAPIC and TEOS are ascribed to the formation of Si–O–Si network structures for the same alkoxy groups of them. A series of luminescent molecular-based hybrid materials were firstly constructed using HIPA-TESPIC coordinated to a different ratio blend of active rare earth ions and inert rare earth ions. As active rare earth ions and inert rare earth ions exist in the same molecule, the fluorescent enhancement effect occurs and is discussed in details. This technology can be expected in the assembly of other luminescent molecular-based hybrid material. In addition, the resulting hybrids could be shaped as monoliths or as transparent films with desired luminescence efficiency.

### Acknowledgements

This work was supported by the National Natural Science Foundation of China (20671072).

### References

- [1] T. Suratwala, Z. Gardlund, K. Davidson, D.R. Uhlmann, *Chem. Mater.* 10 (1998) 190.
- [2] C. Molina, K. Dahmouche, C.V. Santilli, *Chem. Mater.* 13 (2001) 2818.
- [3] L.R. Matthews, E.T. Knobbe, *Chem. Mater.* 5 (1993) 1697.
- [4] B. Menaa, M. Takahashi, Y. Tokuda, T. Yoko, *Opt. Mater.* 29 (2007) 806.
- [5] M. Casalboni, R. Senesi, P. Propositio, *Appl. Phys. Lett.* 30 (1997) 2969.
- [6] B. Lebeau, C.E. Fowler, S.R. Hall, *J. Mater. Chem.* 9 (1999) 2279.
- [7] P. Innocenzi, H. Kozuka, T.J. Yoko, *J. Phys. Chem. B.* 101 (1997) 2285.
- [8] K. Mstui, F. Momose, *Chem. Mater.* 9 (1997) 2588.
- [9] C. Sanchez, F. Ribot, *New J. Chem.* 18 (1994) 1007.
- [10] J.H. Harreld, A. Esaki, G.D. Stucky, *Chem. Mater.* 15 (2003) 3481.
- [11] P.N. Minoofar, R. Hernandez, S. Chia, B. Dunn, J.I. Zink, A.C. Franville, *J. Am. Chem. Soc.* 124 (2002) 14388.
- [12] J. Choi, R. Tamaki, S.G. Kim, R.M. Laine, *Chem. Mater.* 15 (2003) 3365.
- [13] A.C. Franville, D. Zambon, R. Mahiou, S. Chou, Y. Troin, J.C. Cousseins, *J. Alloys Compd.* 275–277 (1998) 831.
- [14] A.C. Franville, R. Mahiou, D. Zambon, J.C. Cousseins, *Solid State Sci.* 3 (2001) 211.
- [15] M. Kawa, J.M.J. Frechet, *Chem. Mater.* 10 (1998) 286.
- [16] H.R. Li, L.S. Fu, H.J. Zhang, *Thin Solid Films* 416 (2002) 197.
- [17] H.R. Li, J. Lin, H.J. Zhang, L.S. Fu, *Chem. Commun.* (2001) 1212.
- [18] D.W. Dong, S.C. Jiang, Y.F. Men, X.L. Ji, B.Z. Jiang, *Adv. Mater.* 12 (2000) 646.
- [19] F.Y. Liu, L.S. Fu, H.J. Zhang, *New J. Chem.* 27 (2003) 233.
- [20] A.C. Franville, D. Zambon, R. Mahiou, *Chem. Mater.* 12 (2000) 428.
- [21] S.T. Hobson, K.J. Shea, *Chem. Mater.* 9 (1997) 616.
- [22] Q.M. Wang, B. Yan, *J. Mater. Chem.* 14 (2004) 2450.
- [23] M. Nandi, J.A. Conklin, L. Salvati, A. Sen, *Chem. Mater.* 2 (1990) 772.
- [24] F.Y. Liu, L.S. Fu, H.J. Zhang, *New J. Chem.* 27 (2003) 233.
- [25] Q.M. Wang, B. Yan, *Inorg. Chem. Commun.* 7 (2004) 747.
- [26] Q.M. Wang, B. Yan, *Inorg. Chem. Commun.* 7 (2004) 1124.
- [27] Y.Y. Xu, I. Hemmilla, *Anal. Chem. Acta* 9 (1992) 256.
- [28] S. Sato, M. Wada, *Bull. Chem. Soc. Jpn.* 43 (1970) 1955.
- [29] B. Yan, Y.S. Song, *J. Lumin.* 14 (2004) 289.
- [30] Q.M. Wang, B. Yan, *Cryst. Growth Design* 5 (2005) 497.